New sulfonic acid moiety grafted on montmorillonite as filler of organic–inorganic composite membrane for non-humidified proton-exchange membrane fuel cells

Youngkwon Kim [a], Younggeun Choi [a], Hae Kyoung Kim [b], Jae Sung Lee [a],*

[a] Eco-friendly Catalysis and Energy Laboratory (NRL), School of Environmental Engineering and Department of Chemical Engineering, Pohang University of Science and Technology, San 31 Hyoja-Dong, Pohang 790-784, Republic of Korea
[b] School of Materials Science & Engineering, Yeungnam University, Gyeongsan 712-749, Republic of Korea

ABSTRACT

A new organic sulfonic acid moiety is grafted on the surface of montmorillonite (MMT) by a condensation reaction of the surface hydroxyl group of MMT with the thiol group of 3-mercaptopropyltrimethoxy silane (3-MPTMS), and simultaneously attaching sulfonic acid group by a ring opening reaction of 1,3-propane sultone. The new method produces MMT functionalized with sulfonic acid of a longer chain length in a simple one-step reaction and shows higher ion-exchange capacity and thermal stability than MMT grafted by a two-step method of 3-MPTMS condensation followed by oxidation with H_2O_2. Using these functionalized MMTs as inorganic fillers, organic–inorganic composite, proton-conducting membranes are cast together with Nafion®. The composite membrane with MMT grafted with the long-chain sulfonic acid shows increased water uptake, while maintaining comparable ionic conductivity relative to a pristine Nafion membrane. This leads to much enhanced performance of a proton-exchange membrane fuel cell without external humidification of reactant gases. For instance, the current density at 0.5 V of the membrane–electrode assembly (MEA) fabricated with a composite membrane containing MMT with the long-chain organic sulfonic acid is about twice that of a MEA fabricated with a composite membrane containing MMT with short-chain organic sulfonic acids and about three times higher than that with pristine Nafion 212.

© 2010 Elsevier B.V. All rights reserved.

1. Introduction

Proton-exchange membrane fuel cells (PEMFCs) have wide application that include road vehicles and residential heat/power supplies [1]. Two key components that determine the performance and cost of PEMFCs are the electrocatalysts and the proton-exchange membrane (PEM). The latter is employed to provide proton conduction from the anode to the cathode, and to separate the anode (hydrogen) and cathode (oxygen) reactants. Perfluorinated sulfonic acid resin (such as Nafion®) is the most common PEM and must be kept well hydrated to retain acceptable proton conductivity. Loss of water content in the PEM leads to a sharp decrease in the proton conductivity and to shrinkage of the membrane. The latter results in mechanical degradation of the membrane|catalyst interface. It is obviously desirable to run PEMFCs without externally humidifying the reactant gases—this reduces cost, size and complexity. For this purpose, it is vital to improve the proton conductivity of PEMs under conditions of low humidity [2].

A common strategy that has been adopted to improve the water retention capacity is to integrate hygroscopic materials in the membranes [3–5]. A layered clay family is a promising candidate for the hybrid fuel cell membrane to obtain a hygroscopic property as well as the possible enhancement of thermal, mechanical and barrier properties. The composite membranes have been prepared mostly by addition of MMT in the Nafion® membrane to reduce the methanol permeability through the polymer electrolyte membrane in direct methanol fuel cells (DMFCs) [6–10]. These composite membranes containing inorganic moieties did not, however, always lead to the desired improvement in the performance of the membrane–electrode assembly (MEA), mainly because the proton conductivity of the composite membranes containing these less-proton-conductive oxides was markedly lowered compared with that of a pristine Nafion® membrane.

Organically modified MMT has an improved capability of dispersing, gelling, adsorption and nanocomposite formation in organic systems [11–16]. Styrene sulfonic moieties were bonded with a clay surface via plasma activation and the Nafion/clay-SO_3H composite membrane was studied in comparison with a commercial Nafion membrane [15]. MMT was also modified by dodecylamine to prepare a Nafion composite membrane [16]. The

* Corresponding author. Tel.: +82 54 2792266; fax: +82 54 2795528.
E-mail address: jlee@postech.ac.kr (J.S. Lee).

water retention and proton conductivity of these composite membranes were enhanced and the power density of the fuel cell using a hybrid membrane was significantly improved, especially in dehydrated working conditions. In previous studies [11–13], we modified the surface of montmorillonite (MMT) or TiO_2 with an organic sulfonic acid group and formed composite membranes with Nafion® in order to minimize the loss of proton conductivity caused by adding the non-conducting inorganics while reducing the methanol permeability. Indeed, MEA containing MMT functionalized with organic sulfonic acid groups demonstrated much improved performance from direct methanol fuel cells compared with MEA containing the pristine Nafion membrane or the composite membranes made with unmodified MMT. This functionalization method is commonly employed to render strong acidity to minerals like kaolinite, magadiite and montmorillonite [17–20].

In this work, a new organic sulfonic acid moiety was grafted on the surface of montmorillonite by a condensation reaction of the surface hydroxyl group of MMT with the thiol group of 3-mercaptopropyltrimethoxy silane (3-MPTMS), and simultaneously attaching a sulfonic acid group by a ring opening reaction of 1,3-propane sultone. The new method produced MMT functionalized with sulfonic acid of a longer chain length in a simple one-step reaction and showed higher ion-exchange capacity and thermal stability than MMT grafted by a two-step method of 3-MPTMS condensation followed by oxidation with H_2O_2. Using these functionalized MMTs as inorganic fillers, organic–inorganic composite, proton-conducting membranes were cast together with Nafion®. To obtain efficient nanocomposites, the MMT nanolayers must be uniformly dispersed in the polymer matrix, as opposed to being aggregated as tactoids or simply intercalated [21]. The new organic sulfonic acid moiety has a long-chain length compared with the ones obtained by the conventional two-step reaction. The longer chain length can enhance the interlayer distance of MMT, and promote the intercalation or exfoliation of MMT thereby improving the organic–inorganic interactions. The characteristics of the membrane are studied in terms of water uptake, proton conductivity and spectroscopic properties, and the performance of MEA fabricated from these membranes is evaluated for PEMFC at a non-humidified gas-feeding condition. These are compared with MEAs containing MMT fillers grafted with a short-chain organic sulfonic acid group by the conventional method.

2. Experimental

2.1. Fabrication of functinonalized MMT and composite membranes

Raw MMT (Aldrich, Montmorillonite-K10) was treated with $0.5\,M\ H_2SO_4$ at 338 K to convert Na^+-MMT into H^+-MMT. The surface functionalization of H^+-MMT was performed using the surface hydroxyl groups of MMT by condensation with 3-meraptopropyltrimehoxy silane (3-MPTMS) and then the grafted terminal thiol group was reacted with 1,3-propane sultone (1,3-PS) as a sulfonic acid precursor to render a new organic sulfonic acid moiety with a long-chain length as schematically depicted in Scheme 1. The MMT functionalized with the new organic sulfonic acid (HSO_3-RSR-MMT) was thus made. The reactions were carried out at the refluxing temperature of toluene (383 K) for 6 h with a molar ratio of H^+-MMT, sulfonic acid precursor and toluene of 1:0.5:15. Next, upon addition of the same molar amount of 3-MPTMS and 1,3-PS, the reflux reaction was carried out for 24 h. The prepared sample was separated by filtration, washed with toluene and dried at 383 K in a vacuum oven. For comparison, the conventional two-step method of MMT functionalization is also depicted in Scheme 1 with 3-MPTMS condensation followed by oxidation
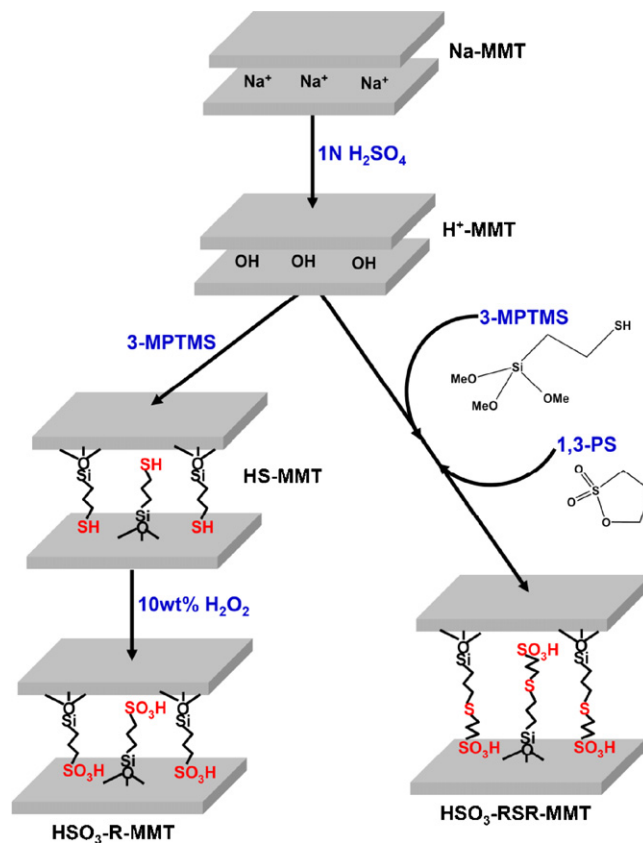
Scheme 1. A schematic representation for the functionalization steps of montmorillonites.

with H_2O_2 (HSO_3-R-MMT). Without addition of 1,3-PS, the chain length (R) is shorter than that obtained by the new method (RSR).

To prepare a composite membrane, 5 wt.% (based on Nafion®) of HSO_3-RSR-MMT or HSO_3-R-MMT was added to a 20 wt.% Nafion solution (Dupont), and then stirred mechanically and degassed by ultrasonication. The prepared mixture was poured on to a glass plate and the composite membrane was cast by the doctor-blade method. The membrane was dried by slowly increasing the temperature from 353 to 403 K to prevent crevices in the composite polymer membrane. Finally, the residual solvent in composite membrane was fully removed by evaporation at 403 K for 12 h. The thickness of the composite membrane was ca. 20 μm. For comparison, a 20 μm Nafion membrane was recast by the same method. All membranes were boiled at 353 K in hydrogen peroxide for 1 h and then rinsed with deionized water. Next, they were immersed in 0.5 M sulfuric acid at 353 K for 2 h to convert membranes to the H^+-form, and then rinsed with deionized water to remove the excess sulfuric acid.

2.2. Physical characterization

X-ray diffraction (XRD) patterns were obtained on a MAC Science Co, M18XHF diffractometer with Cu Kα radiation (40 kV, 200 mA). Thermogravimetric analysis (TGA, TGS-2) was operated in the range of 323–1073 K at a heating rate of $10\,K\,min^{-1}$ under an air flow of $40\,ml\,min^{-1}$. X-ray photoelectron spectra (XPS) were acquired with a VG-Scientific ESCALAB 220 iXL spectrometer equipped with a hemispherical electron analyzer and a Mg Kα (1253.6 eV) X-ray source. The ^{29}Si solid-state NMR measurements were performed on a Varian Unity Inova 300 MHz spectrometer (7.4 T) equipped with a 7 mm Chemagnetics MAS probe head using a sample rotation rate of 5.0 kHz. The spectra of ^{29}Si MAS NMR were

measured at a frequency of 59.590 MHz. Transmission electron microscopy (TEM) images were taken on a Hitachi 7600 operated at 80 kV. TEM samples were prepared by using an Ultra-microtome (RMC MT 7000) with a 45° diamond knife and mounted on a 200 mesh copper grid.

2.3. Ion-exchange capacity measurements

The ion-exchange capacity (IEC) (mmol of sulfonic acid per g of HSO$_3$-RSR-MMT) of each sample was determined by the back-titration method. 0.5 g of the sample was soaked overnight in 50 ml of distilled water containing 5 ml of 0.1N NaOH to exchange sodium ions with the protons in the inorganic. Back-titration was accomplished by titrating the remaining NaOH in solution with 0.1 M HCl solutions. The IEC values were obtained by subtracting the added volume of 0.1 M HCl from the initial NaOH volume.

2.4. Water uptake measurements

The water contents of the membranes were measured in parallel under the same conditions. The membrane samples (3 cm × 3 cm) were dried under vacuum at 333 K for 12 h and weighed prior to testing. They were then immersed in deionized water for 24 h at room temperature to obtain equilibrated water uptake. The gravimetric water uptakes were calculated using the following equation: water uptake % = 100($W_1 - W_0$)/W_0, where W_0 and W_1 are the weight of the membrane before and after water absorption.

2.5. Ionic conductivity measurements

The ionic conductivity of the composite membranes was measured by a 4-point probe method using an *a.c.* impedance analyzer. The composite membrane was fixed in a measuring cell that comprised two outer platinum foils and two inner platinum wires. The installed cell was placed in a chamber with a controlled relative humidity of 98% and temperature range of 300–360 K. By applying constant currents (I) through the two outer Pt-probes and measuring the associated voltage (V) drops across the two inner Pt-probes, the resistance (R) of the membrane was measured. The ionic conductivity (σ) was calculated by $\sigma = L/(A \times R)$, where L and A are the distance between the two inner Pt-probes and the cross-sectional area of the membrane, respectively.

2.6. Performance tests of a single cell

The catalyst slurries for the cathode and the anode were prepared by mixing Pt/C with a 5 wt.% Nafion solution. For fabrication of the membrane–electrode assembly (MEA), the catalyst slurry was coated on a carbon paper substrate. The catalyst loading was approximately 0.5 mg-Pt cm^{-2} for both the anode and the cathode and the effective electrode area of the single cell was 5 cm^2. The MEA was fabricated by hot pressing at 408 K and 1500 psi for 90 s. The performance of the PEMFC was evaluated at 333 K with 60 ml min^{-1} of hydrogen and 180 ml min^{-1} of air without intentional humidification.

3. Results and discussion

3.1. Synthesis and characterization of sulfonated MMTs

A new organic sulfonic acid moiety was grafted on the surface of montmorillonite (MMT) by condensation reaction of the surface hydroxyl group (–SiOH) of MMT with the thiol group of 3-mercaptopropyltrimethoxy silane (3-MPTMS), and simultaneously attaching a sulfonic acid group by a ring opening reaction of 1,3-propane sultone (1,3-PS). This one-step functionalization process
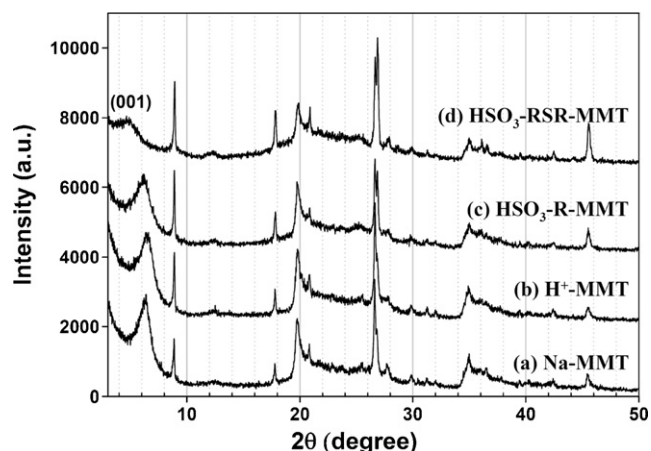

Fig. 1. Wide-angle X-ray diffraction (XRD) patterns of (a) Na-MMT, (b) H$^+$-MMT, (c) HSO$_3$-R-MMT, and (d) HSO$_3$-RSR-MMT.

with a long-chain sulfonic acid moiety is summarized in Scheme 1 and represents a significant advancement over the two-step processes that are commonly used for organic acid functionalization of MMT [11,12]. The two-step process employs silanes (3-MPTMS) as starting materials that produce a thiol group (–SH) moiety (SH-MMT), which is then oxidized with H$_2$O$_2$. The oxidation of this thiol group to sulfonic acid is particularly troublesome due to the large exothermicity of the oxidation reaction and a substantial amount of the grafted surface sulfur species is lost during this process [11]. Thus, the new one-step process simplifies and makes more effective the surface functionalization of MMT in addition to yielding a new organic sulfonic acid moiety of longer chain length.

The XRD patterns of unmodified and sulfonated MMT are compared in Fig. 1. The low-angle XRD peak representing the (0 0 1) plane of Na-MMT and H$^+$-MMT does not change much before or after ion-exchange treatment in Fig. 1(a) and (b) ($2\theta_{Na-MMT}$ = 6.40, $2\theta_{H^+-MMT}$ = 6.44). There is only a slight decrease in the interlayer distance. This indicates that the original structure is well preserved during the acid treatment to place the surface hydroxyl group on the surface of MMT [22]. Upon surface functionalization of H$^+$-MMT with a short-chain sulfonic acid group (HSO$_3$-R-) and a long-chain sulfonic acid group (HSO$_3$-RSR-) and the low-angle XRD peak area shifted from *ca.* 6.44° to 6.10° and to 5.02°, respectively, as shown in Fig. 1(b)–(d). From the Bragg law, the interlayer distance is estimated to increase from 1.37 to 1.45 nm, or 1.76 nm, which indicates that the grafted functional groups (HSO$_3$-R-, HSO$_3$-RSR-) on the surface of MMT increase the interlayer distance of MMT [11]. In particular, the long-chain functionalized MMT (HSO$_3$-RSR-MMT) has a longer interlayer distance compared with the short-chain fucntioalized MMT (HSO$_3$-R-MMT). Thus, as expected, the chain length of functional groups affects the basal spacing of MMT. Further, this long-chain functional group is better intercalated into the MMT valley, as indicated by the much reduced intensity of the (0 0 1) diffraction peak.

The ion-exchange capacity (IEC, mmol of sulfonic acid per g of HSO$_3$–MMT) is an important factor determining ion conductivity. Thus the IEC of each sample was determined by the back-titration method [11–13] and the results are given in Fig. 2. The H$^+$-MMT sample treated with 0.5 M H$_2$SO$_4$ shows an initial pH of 4.9 and an IEC of 0.31 mmol g^{-1}, which indicates that Na$^+$ in the interlayer of MMT has exchanged with H$^+$. The HSO$_3$-RSR-MMT sample has the lowest pH and highest IEC values (0.64 mmol g^{-1}) among all samples, followed by HSO$_3$-R-MMT (0.52 mmol g^{-1}) and H$^+$-MMT (0.46 mmol g^{-1}).

In Fig. 3, X-ray photoelectron spectra (XPS) of S 2p core level for the *in situ* outgassed samples reveal characteristic S2p$_{3/2}$–S2p$_{1/2}$
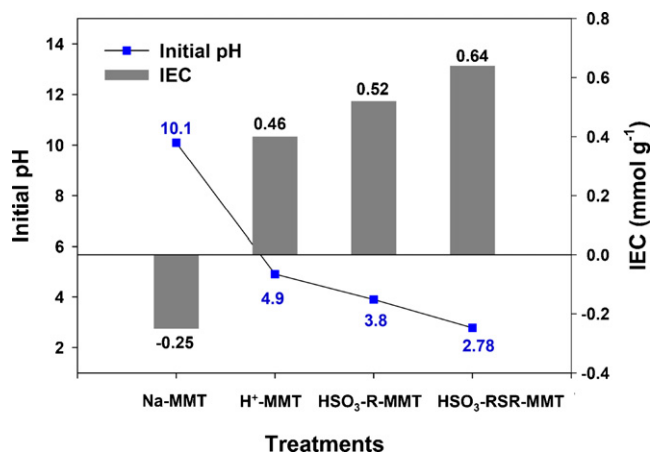
Fig. 2. pH and ion-exchange capacities (IEC) of montmorillonites upon grafting precursors.

spin–orbital splitting. The XPS analysis is useful for evaluating qualitatively the type of sulfur species and measuring quantitatively the sulfonic acid groups near the surface region [11–13]. The chemical properties of the samples were probed by examining the more intense component S2p$_{3/2}$. Samples show two types of sulfur species: one at low binding energy (BE), *ca.* 163.2 eV, corresponding to S^{2-} species due to alkyl sulfide (R-S-R') or thiol (–SH) groups, and the other at a higher BE, *ca.* 168.0 eV, associated with a sulfate (S^{6+}) species due to sulfonic (–SO$_3$H) group [23]. This energy difference in XPS analysis between S^{2-} and S^{6+} makes a useful tool for evaluating the degree of sulfonation near the surface region. Thus, considering the intensity of S^{6+} peaks in Fig. 3 for each HSO$_3$-MMT sample, we can conclude that the long-chain organic sulfonic functional group (HSO$_3$-RSR-) is more efficiently grafted on to the surface of MMT than the shorter functional group (HSO$_3$-R-). The surface concentration of the sulfonic acid moiety was estimated from the intensity of these sulfur XPS peaks relative to that of Si peak, notwithstanding the inaccuracy involved in comparison of XPS peak intensities between different samples. As shown in Fig. 3, most thiol groups in the SH-MMT sample are converted into sulfonic acid groups by oxidation with 10 wt.% H$_2$O$_2$ at 333 K with only *ca.* 6% of the thiol groups remaining in an unoxidized form. By contrast, total amount of residual sulfur is *ca.* 60%, compared with the sulfur content of the sample before oxidation. In MMT with the long-chain organic sulfonic acid, sulfonic acid groups are bonded to the thiol group of
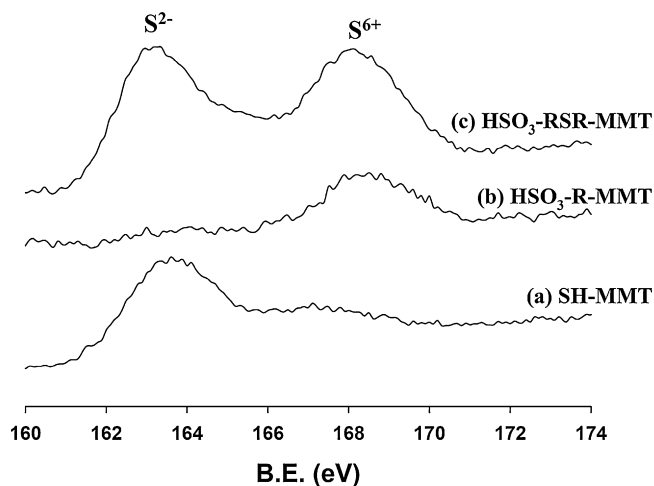

Fig. 3. X-ray photoelectron spectra (XPS) in S 2p core level region of (a) HS-MMT, (b) HSO$_3$-R-MMT, and (c) HSO$_3$-RSR-MMT.
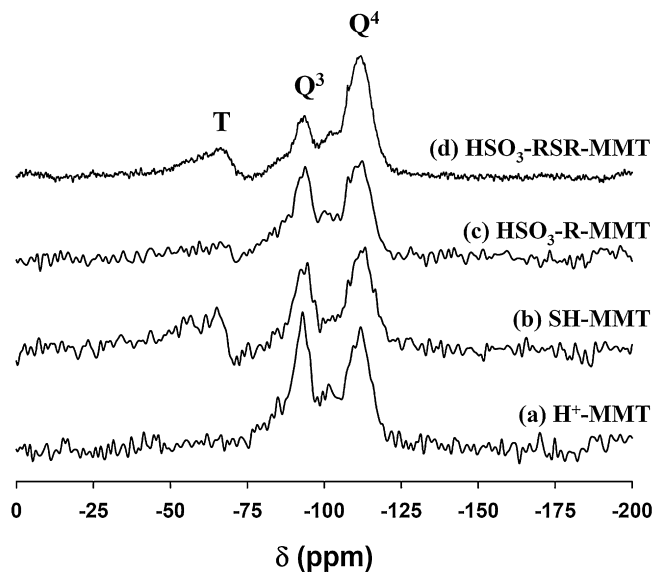

Fig. 4. ^{29}Si MAS NMR spectra of (a) H$^+$-MMT, (b) HS-MMT, (c) HSO$_3$-R-MMT, and (d) HSO$_3$-RSR-MMT.

SH-MMT, thus comparable intensities of S^{2-} and S^{6+} are observed. The HSO$_3$-RSR-MMT sample shows no loss of S^{2-} species compared with SH-MMT and exhibits a much higher intensity of S^{6+} species in comparison with HSO$_3$-R-MMT.

^{29}Si MAS NMR spectroscopy is useful for the study of layered aluminosilicate minerals to determine the local structure around Al and Si atoms [24,25], and for examining silyated compounds [26,27]. In general, MMT exhibits a resonance in the range of −75 to −120 ppm, as shown in Fig. 4. Each Si atom in MMT structures has two or three Si atoms as nearest neighbors and the remaining nearest neighboring atoms are either Al or H. The Q^3 is attributed to central Si in (Si–O–)$_2$Si(–O–Al)–OH and Q^4 in (Si–O–)$_3$Si(–O–Al) [11,28]. H$^+$-MMT exhibits ^{29}Si responses in the range of −75 to −120 ppm as shown in Fig. 4(a). After the surface functionalization with 3-MPTMS, two changes are noticed in Fig. 4(b); a new broad peak (T) appears near −50 to −70 ppm. This new peak (T) is due to the silane species grafted on the surface and in accord with the reported Si signal for alkyltrimethoxysilane or alkyltrichlorosilane grafted on layered silicates (near −55 to −65 ppm) [11,12,26,27]. Thus, the Si atom is covalently bonded to carbon (–O$_3$Si–CH– species). The intensity of the new peak (T) decreases when HS-MMT is treated with hydrogen peroxide to oxidize the thiol group. This indicates that a large portion of grafted 3-MPTMS molecules becomes detached from the silicate surface. There is no significant change in the Q^3, Q^4 parts of the spectrum. After the surface functionalization, the increase of the Q^4/Q^3 ratio compared with unfunctionalized MMT clearly indicates the successful grafting of different sulfonic acid moieties to the surface silanol group. Especially, the higher Q^4/Q^3 value of HSO$_3$-RSR-MMT compared with that of HSO$_3$-R-MMT indicates that the long-chain functional group has been more efficiently grafted on the MMT surface than the short-chain functional group. These results of ^{29}Si MAS NMR are consistent with the results described above based on XRD, XPS, and IEC analysis.

The thermal stability of functionalized MMT with different organic chain lengths was studied by thermogravimetric analysis (TGA) as shown in Fig. 5. Normally, MMT does not change thermally in the temperature range of 443–773 K, so that the weight loss over this temperature range should come from the decomposition and/or evaporation of the organic moieties [29]. The weight losses of all samples in the temperature range from 323 to 425 K are *ca.* 2–4 wt.%, and are probably caused by loss of water contained in
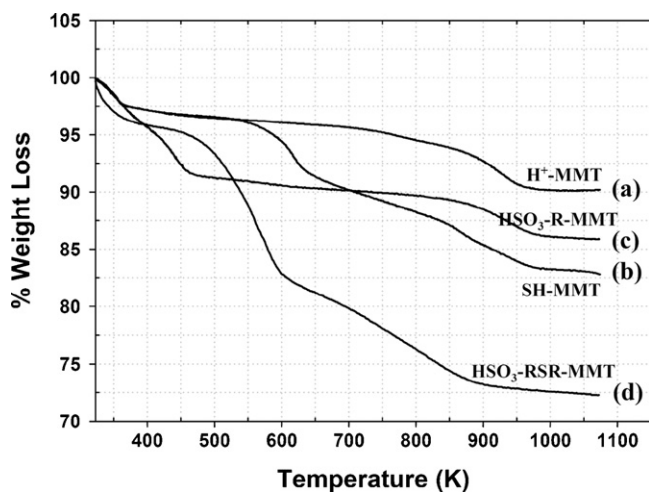
Fig. 5. Thermogravimetric analysis (TGA) curves of (a) H$^+$-MMT, (b) HS-MMT, (c) HSO$_3$-R-MMT, and (d) HSO$_3$-RSR-MMT.

the interlayers. As shown in Fig. 5(b), a weight loss of *ca.* 6 wt.% is recorded for SH-MMT between 533 and 673 K because the surface functionalized thiol group is thermally decomposed; eventually, the sample loses 17% of its initial weight at 1073 K. For HSO$_3$-R-MMT, a weight loss of *ca.* 6 wt.% shown in Fig. 5(c) is recorded between 373 and 453 K because the sulfonic acid group is thermally cracked in this temperature region; the eventual weight loss is *ca.* 14%. In the case of HSO$_3$-RSR-MMT shown in Fig. 5(d), a weight loss of *ca.* 13% is recorded between 425 and 580 K because the sulfonic acid group and alkyl sulfide group are thermally cracked throughout this region; the eventual weight loss is *ca.* 27%. In any case, the thermal stability of the sulfonic acid groups would limit the allowed operating temperature of these materials. Fortunately, however,

the decomposition temperatures are all much higher than the usual operating temperatures of DMFC (<353 K) and PEMFC (<373 K). This thermal stability is also better than HSO$_3$-MMT functionalized by the previous two-step method as these suffer decomposition of the sulfonic acid group below 400 K [11].

3.2. Nafion/sulfonated MMT nanocomposite membranes

Nafion/sulfonated MMT composite and recast Nafion membranes were cast by the doctor-blade method. The thickness of the cast membranes was *ca.* 20 μm. Wide-angle XRD patterns of a surface functionalized MMT/Nafion composite membranes are shown in Fig. 6A and B. The absence of the diffraction peak of the (0 0 1) plane for the HSO$_3$-RSR-MMT/Nafion composite membranes in Fig. 6A(d) and B indicates that the sulfonated MMT has lost the regularity of its layered structure in the Nafion matrix [30]. On the other hand, 5 wt.% H$^+$-MMT/Nafion and 5 wt.% HSO$_3$-R-MMT/Nafion composite membranes in Fig. 6A(b, c) show the characteristic (0 0 1) crystal plane of MMT. The low-angle peak of a 5 wt.% HSO$_3$-R-MMT/Nafion composite membrane is shifted to a lower 2θ angle in comparison with that of a 5 wt.% H$^+$-MMT/Nafion composite membrane. This is due to the increased interlayer distance of HSO$_3$-R-MMT caused by the orgnic sulfonated surface functional group as shown in Fig. 1(c). In the case of the 5 wt.% HSO$_3$-RSR-MMT/Nafion composite membrane shown in Fig. 6A(d), the low-angle XRD peak disappears probably because of the higher interlayer distance of HSO$_3$-RSR-MMT due to the increased chain length of the organic sulfonic acid functional group as shown in Fig. 1(d). Fig. 6(B) shows the wide-angle XRD patterns of HSO$_3$-RSR-MMT/Nafion composite membranes with different inorganic contents (1–10 wt.%). The XRD pattern of a 10 wt.% HSO$_3$-RSR-MMT/Nafion composite membrane (Fig. 6B(d)) shows a decreased peak intensity at 2θ = 12–17°, which can be deconvoluted into two peaks (2θ = 16° and 17.5°) and attributed to amorphous and
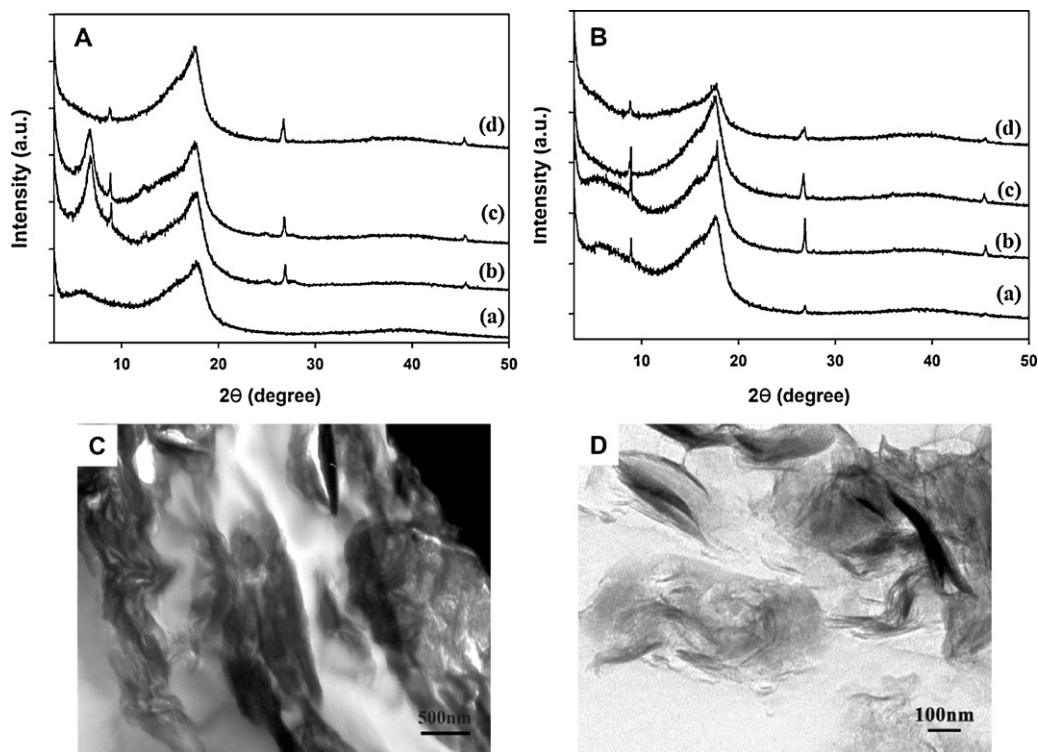

Fig. 6. (A) Wide-angle X-ray diffraction (WXRD) patterns: (a) recast Nafion membrane, (b) 5 wt.% H$^+$-MMT/Nafion, (c) HSO$_3$-R-MMT/Nafion, and (d) HSO$_3$-RSR-MMT/Nafion composite membranes. (B) WXRD of composite membrane with different HSO$_3$-RSR-MMT contents: (a) 1 wt.%, (b) 3 wt.%, (c) 5 wt.%, and (d) 10 wt.%. Transmission electron microscope (TEM) image of 5 wt.% HSO$_3$-R-MMT/Nafion (C) and 5 wt.% HSO$_3$-RSR-MMT/Nafion (D) composite membranes.

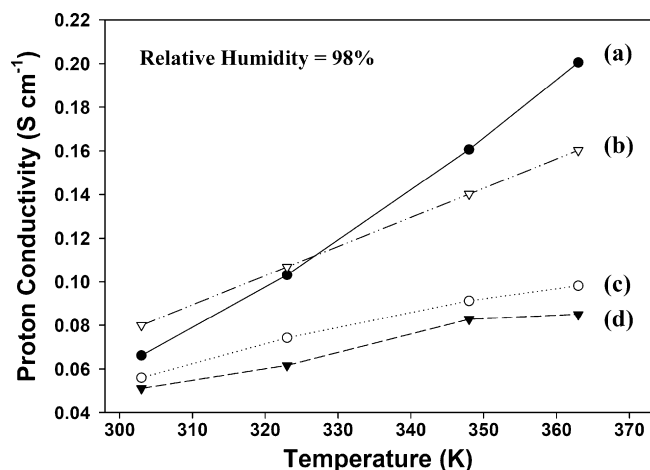**Fig. 7.** Proton conductivity of (a) recast Nafion, (b) 5 wt.% HSO$_3$-RSR-MMT/Nafion, (c) 5 wt.% HSO$_3$-R-MMT/Nafion, and (d) 5 wt.% H$^+$-MMT/Nafion composite membranes. Conductivity measured at relative humidity of 98% and over temperature range of 300–360 K. All membranes have same thickness of *ca.* 20 μm.

Fig. 8. Water uptake (%) of recast Nafion and composite membranes containing 5 wt.% inorganics.

crystalline scattering from the polyfluorocarbon chains of Nafion [31,32]. This can be understood by the larger amount of functionalized MMT that blocks the cross-linking process of the Nafion ionomer. The TEM images of the 5 wt.% short-chain and long-chain functionalized MMT/Nafion composite membranes are presented in Fig. 6(C) and (D). The 5 wt.% HSO$_3$-RSR-MMT/Nafion composite membrane in Fig. 6(D) shows reduced regularity of MMT compared with that of 5 wt.% HSO$_3$-R-MMT/Nafion composite membrane. The TEM image of 5 wt.% HSO$_3$-R-MMT/Nafion composite membrane, however, indicates that the majority of the inorganic fillers still maintain the layered structure although the structural regularity has became very low. Some thin layers or plates are also seen. Thus, the interaction between MMT and Nafion is mostly intercalation in nature with a small degree of exfoliation.

The proton conductivities of a pristine Nafion membrane and the composite membranes measured at the relative humidity of 98% and temperature range of 300–360 K are shown in Fig. 7. The thickness of all the composite membranes was kept at *ca.* 20 μm by employing a doctor-blade method. The proton conductivity of the composite membranes was measured by the *a.c.* 4-point probe method using an a.c. impedance analyzer. As shown, the proton conductivities of unfunctionalized MMT/Nafion composite membranes in Fig. 7(b) are lower than those of Nafion in Fig. 7(a) and the other surface functionalized MMT/Nafion composite membranes. The ionic conductivity of the 5 wt.% HSO$_3$-R-MMT/Nafion membrane in Fig. 7(c) is slightly higher than that of the unfunctionalized MMT/Nafion composite membrane but much lower than that of Nafion 212. On the other hand, the ionic conductivity values of the composite membrane containing 5 wt.% HSO$_3$-RSR-MMT are higher than that of Nafion below at 323 K, and only slightly lower than Nafion above 323 K. The other two composite membranes containing 5 wt.% of HSO$_3$-R-MMT and H$^+$-MMT have much lower ionic conductivities than Nafion 212 at all temperatures.

The water contents of recast Nafion and composite membranes are given in Fig. 8. The samples for these tests had the same size (3 cm × 3 cm) and were prepared under the same conditions. Surface functionalized MMT/Nafion composite membranes show higher water uptake than the unfunctionalized MMT/Nafion composite membrane and recast Nafion membrane, but the unfunctionalized MMT/Nafion composite membrane has lower water uptake than recast Nafion. Especially, 5 wt.% HSO$_3$-RSR-MMT/Nafion composite membrane has the highest water capacity among all other membranes. This result implies that the water uptake ability of a composite membrane depends on the nature
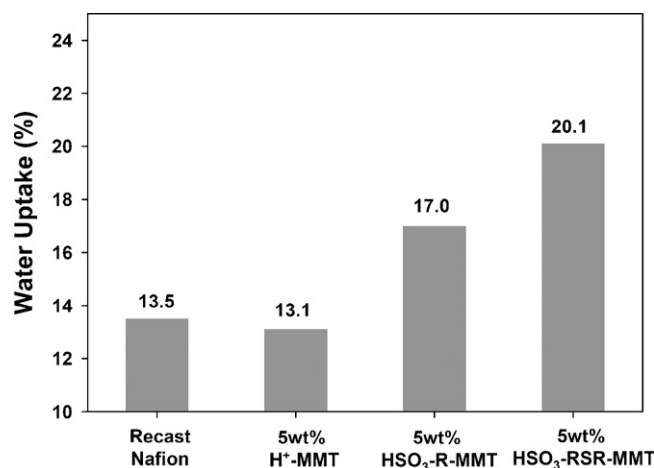
of the surface functional group of the inorganic filler. The highest water content of the 5 wt.% HSO$_3$-RSR-MMT/Nafion composite membrane may be related to the high IEC value and large interlayer distance of MMT introduced by the long-chain sulfonic acid functional group. Water content in the membrane is an important parameter for PEMFCs in low humidity or dry operation. The ionic conductivity of the membrane also depends highly on the relative humidity [2].

Fig. 9 gives the performance under PEMFC operating conditions of single cells containing a MEAs made with composite membranes of different inorganic materials, pristine Nafion 212, and recast Nafion. The same 20 wt.% Pt/C catalyst is employed for the electrodes of the MEAs and the amount of electrode catalysts is 0.5 mg-Pt cm^{-2}. The composite membrane with 5 wt.% HSO$_3$-RSR-MMT displays much improved performance relative to that of Nafion 212 itself in a non-humidified gas-feeding condition. By contrast, the composite membrane with 5 wt.% H$^+$-MMT with no sulfonic acid groups does not give any performance of a PEMFC in non-humidified gas-feeding operation. The voltage drop in the low current density region of the *I–V* curve reflects the activation loss for O$_2$ reduction [33]. The low open-circuit voltage (OCV) of around 0.9 V is well below that of the theoretical voltage of 1.23 V due to the drastic loss of activation and loss of gas permeability through the membrane. In Fig. 9, MEAs containing recast Nafion (thickness = *ca.* 20 μm) and Nafion 212 (thickness = *ca.* 50 μm) show
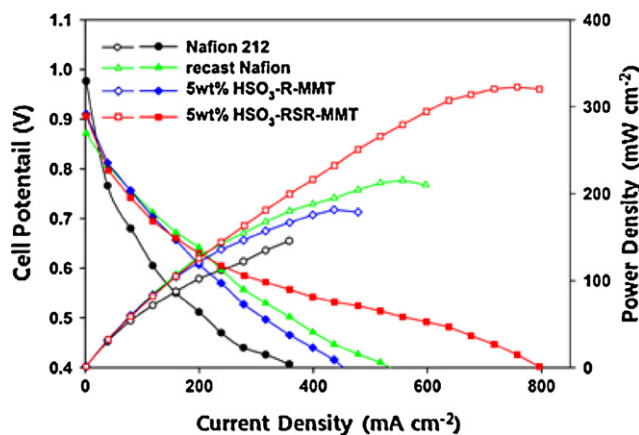

Fig. 9. Polarization curves of MEA made with Nafion 212 (thickness ~50 μm), recast Nafion and composite membranes (thickness ~20 μm) operated at 333 K. Flow rate of dry H$_2$ = 60 ml min^{-1} and dry air = 180 ml min^{-1}.

similar OCV values (*ca.* 0.9 V). Thus, the reduced thickness of the membrane does not affect OCV loss by gas permeability through the membrane.

The power densities measured with the composite membranes with 5 wt.% inorganic fillers of HSO_3-R-MMT, and HSO_3-RSR-MMT are 157 and 290 mW cm^{-2}, respectively, at a potential of 0.5 V. By comparison, the power density measured with Nafion 212 and recast Nafion membranes are 102 and 180 mW cm^{-2}, respectively, at a potential of 0.5 V. The power density of the MEA fabricated with HSO_3-RSR-MMT/Nafion composite membrane is *ca.* 2 times higher than that of the MEA fabricated with HSO_3-R-MMT/Nafion and *ca.* 3 times higher than that with pristine Nafion 212. To study the effect of the thickness of the membrane, a recast membrane of *ca.* 20 μm thickness was prepared. The performance of the MEA containing the recast Nafion membrane was better than that of the Nafion 212 and HSO_3-R-MMT/Nafion composite membranes, but much worse than that of the HSO_3-RSR-MMT/Nafion composite membrane. A reduction in membrane thickness can enhance back-diffusion of water from the cathode and thus alleviate the water-management problem [34]. Since the HSO_3-RSR-MMT/Nafion membrane has the same thickness as that of the recast Nafion membrane, however, the best performance with the HSO_3-RSR-MMT/Nafion composite membrane should be due to its higher water uptake capability compared with recast Nafion, and its higher proton conductivity compared with the other composite membranes.

There have been many attempts to improve the cell efficiency of PEMFCs that operate with a dry gas feed through incorporation of inorganic moieties into Nafion membrane [3–5]. To date, however little success has been reported that meets the expectations put into these composite membranes. This is mainly because the ion conductivity of the composite membrane is lowered to an unacceptable level. To increase the ionic conductivity of composite membranes, the surface functionalization of MMT has been performed by two-step functionalization with short-chain organic sulfonic acids [11–13]. Relative to the conventional method of functionalization, the new method employed in the present study is simpler and provides higher interlayer distance of MMT and higher ionic conductivities. In particular, the 5 wt.% HSO_3-RSR-MMT/Nafion composite membrane shows a higher ionic conductivity than that of the pristine Nafion membrane, particularly below 323 K. This excellent proton conductivity appears to be due to the higher content of terminal sulfonic acid functional groups and an improved interaction between the inorganic material and polymer by intercalation of polymer into the MMT valley. Furthermore, the new version of HSO_3-modified MMT shows much improved thermal stability relative to MMT modified with short-chain organic sulfonic acid functional groups.

4. Conclusions

A new method of surface functionalization of montmorillonite with long-chain organic sulfonic acid is found to serve as an effective filler for a composite membrane with Nafion. Relative to the known method, the new method produces materials with higher ion-exchange capacity and thermal stability. The fabricated organic–inorganic composite membrane shows enhanced water uptake, and maintains an ionic conductivity comparable with that of a pristine Nafion membrane. This leads to a much enhanced performance from a PEMFC without external humidification that employs a composite membrane containing MMT grafted with a long-chain organic acid relative to that with a short-chain organic acid or a pristine Nafion membrane.

References

[1] X.G. Yang, C.Y. Wang, Appl. Phys. Lett. 86 (2005) 224104.
[2] J. Yang, P.K. Shen, J. Varcoe, Z. Wei, J. Power Sources 189 (2009) 1016–1019.
[3] K. Kanamura, T. Mitsui, H. Munakata, Chem. Mater. 17 (2005) 4845–4851.
[4] J.D. Halla, M. Mamak, D.E. Williams, G.A. Ozin, Adv. Funct. Mater. 13 (2003) 133–138.
[5] A.B. Bourlinos, K. Raman, R. Herrera, Q. Zhang, L.A. Archer, E.P. Giannelis, J. Am. Chem. Soc. 126 (2004) 15358–15359.
[6] J.M. Thomassin, C. Pagnoulle, G. Caldarella, A. Germain, R. Jérôme, J. Membr. Sci. 270 (2006) 50–56.
[7] J.M. Thomassin, C. Pagnoulle, D. Bizzari, G. Caldarella, A. Germain, R. Jérôme, Solid State Ionics 177 (2006) 1137–1144.
[8] R.K. Bharadwaj, Macromolecules 34 (2001) 9189–9192.
[9] J.M. Thomassin, C. Pagnoulle, G. Caldarella, A. Germain, R. Jérôme, Polymer 46 (2005) 11389–11395.
[10] D.H. Jung, S.Y. Cho, D.H. Peck, D.R. Shin, J.S. Kim, J. Power Sources 118 (2003) 205–211.
[11] C.H. Rhee, H.K. Kim, H. Chang, J.S. Lee, Chem. Mater. 17 (2005) 1691–1697.
[12] C.H. Rhee, Y. Kim, H.K. Kim, H. Chang, J.S. Lee, J. Power Sources 159 (2006) 1015–1024.
[13] Y. Kim, C.H. Rhee, H.K. Kim, H. Chang, J.S. Lee, J. Power Sources 162 (2006) 180–185.
[14] T.K. Kim, M. Kang, Y.S. Choi, H.K. Kim, W. Lee, H. Chang, D. Seung, J. Power Sources 165 (2007) 1–8.
[15] P. Bebin, M. Caravanier, H. Galiano, J. Membr. Sci. 278 (2006) 35–42.
[16] X. He, H. Tang, M. Pan, J. Appl. Polym. Sci. 108 (2008) 529–534.
[17] J.J. Tunney, C. Detellier, Chem. Mater. 5 (1993) 747–748.
[18] E. Ruiz-Hitzky, J.M. Rojo, Nature 287 (1980) 28–30.
[19] T. Yanagisawa, K. Kuroda, C. Kato, React. Solids 5 (1988) 167–175.
[20] L. Merier, C. Detellier, Environ. Sci. Technol. 29 (1995) 1318–1323.
[21] P.C. LeBaron, Z. Wang, T.J. Pinnavaia, Appl. Clay Sci. 15 (1999) 11–29.
[22] O.Y. Kwon, K.W. Park, S.Y. Jeong, Bull. Korean Chem. Soc. 22 (2001) 678–684.
[23] E. Cano-Serrano, G. Blanco-Brieva, J.M. Campos-Martin, J.L.G. Fierro, Langmuir 19 (2003) 7621–7627.
[24] K. Okada, N. Arimitsu, Y. Kameshima, A. Nakajima, K.J.D. MacKenzie, Appl. Clay Sci. 31 (2006) 185–193.
[25] M. Reinholdt, J. Miche-Brendle, L. Delmotte, M.H. Tuilier, R. Le Dred, R. Cortes, A.M. Flank, Eur. J. Inorg. Chem. (2001) 2831–2841.
[26] P.H. Thiesen, K. Beneke, G. Lagaly, J. Mater. Chem. 12 (2002) 3010–3015.
[27] A. Shimojima, D. Mochizuki, K. Kuroda, Chem. Mater. 13 (2001) 3603–3609.
[28] D. Margolese, J.A. Melero, S.C. Christiansen, B.F. Chmelka, G.D. Stucky, Chem. Mater. 12 (2000) 2448–2459.
[29] Y. Xi, R.L. Frost, H. He, T. Kloprogge, T. Bostrom, Langmuir 21 (2005) 8675–8680.
[30] Q.H. Zeng, D.Z. Wang, A.B. Yu, G.Q. Lu, Nanotechnology 13 (2002) 549–553.
[31] P.L. Antonucci, A.S. Arico, P. Creti, E. Ramunni, V. Antonucci, Solid State Ionics 125 (1999) 431–437.
[32] P. Dimitrova, K.A. Freidrich, U. Stimming, B. Vogt, Solid State Ionics 150 (2002) 115–122.
[33] Z. Liu, X. Lin, J.Y. Lee, W. Zhang, M. Han, L.M. Gan, Langmuir 18 (2002) 4054–4060.
[34] H.P. Dhar, US Patent 5,318,863 (1994).